Influence of the gun barrel straightness on projectile exit conditions

M. LIENNARD[a], O. CHEVALIER[b], A. LANGLET[c], Y. GUILMARD[d] and P. BAILLY[e]

a. Laboratoire PRISME de l'Université d'Orléans et Nexter Systems, mathilda.liennard@etu.univ-orleans.fr
b. Nexter Systems, o.chevalier@nexter-group.fr
c. Laboratoire PRISME de l'Université d'Orléans, andre.langlet@ univ-orleans.fr
d. Nexter Systems, y.guilmard@nexter-group.fr
e. Laboratoire PRISME de l'Université d'Orléans, patrice.bailly@insa-cvl.fr

Abstract:

Gun accuracy is influenced by several parameters during the internal ballistics phase. Accuracy is defined by the bias and dispersion of impact points on the target. The aim of this study is to determine the influence of gun barrel straightness on projectile exit conditions, in order to understand how to improve weapon accuracy. A numerical firing analysis was carried out with LS-Dyna software. The model validity is proven by its ability to accurately predict the measured circumferential strains caused by the forcing effect of the projectile, and by the consistency of the contact forces at the projectile-tube interface. To validate the firing simulation, circumferential strains of the tube were measured and compared to LS-Dyna results. Subsequently, the barrel geometry was modified to add a straightness defect to the initial curvature due to gravity. Lastly, a post-treatment was performed to determine the angular and transverse velocities of the projectile during internal ballistics phase.This analysis shown the influence of specific shapes on ammunition balloting and velocity.

Keywords: Gun barrel / accuracy / internal ballistics / numerical analysis / straightness

1 Introduction (16 gras)

Gun accuracy is influenced by several parameters during projectile travel. In the present study, only the internal ballistics phase is considered. Accuracy is defined by the bias and dispersion of impact points on the target. According to previous studies, these parameters are influenced by ammunition design, tube and weapon geometry, and propulsive powder quantity [1]. Experiments performed to determine the effects of these factors on gun barrel performances made it possible to infer a reliable predictive model of the ammunition flight. Using this model, several parameters were improved to increase weapon accuracy.

In order to understand the influence of gun tube geometry on accuracy, a statistical analysis using the data base of firing results of the medium caliber gun was conducted here. The impact of different

parameters was estimated from calculation of the correlation coefficients, following a method similar to that used in [2]. In the latter study, the concentricity between the peaks and groove troughs, some play in the gun, and certain characteristics of the barrel shapes were observed. It was found that defects in barrel straightness appear to significantly affect accuracy. This was confirmed by the results reported in [3], which showed that straightness defects contribute to projectile balloting, i.e., the small oscillations both in translation and rotation undergone by the projectile while traveling through the gun tube. When the projectile exits the tube, balloting affects the muzzle crossing velocity of the ammunition and hence influences initial conditions of the flight phase of the projectile [4]. Thus a high degree of balloting decreases the accuracy and increases dispersion on the target.
The distance between aim point and target impact is named total jump. An American study calculated total jump of the 155 mm M198 Howitzer to identify and possibly improve the largest contributors to jump [5]. In the study, the following equation was developed to compute the aerodynamic jump, J_A, using the exit conditions of the projectile:

$$J_A = {k_t}^2 \times \frac{C_{L\alpha}}{C_{M\alpha}} \times ({\xi_0}' - iP\xi_0)$$

with:

- k_t the sub-projectile transverse radius of gyration;
- $C_{M\alpha}$ the sub-projectile pitching moment coefficient;
- $C_{L\alpha}$ the projectile lift coefficient;
- P a scaled spin rate;
- ξ_0 and ${\xi_0}'$ are the initial sub-projectile complex yaw angle and transverse angular rate evaluated at the muzzle, respectively.

It was concluded that the main contributor to total jump is the CG-jump, which is the angular deviation of the projectile at the muzzle relative to the instantaneous muzzle center line at shot exit. CG-jump is obtained by subtracting the sum of the muzzle crossing velocity components from the initial projectile trajectory angle. Muzzle crossing velocity is the angle formed by the ratio of the gun muzzle transverse velocity at the instant of shot exit to the projectile exit velocity.
In order to understand the effect of different barrel shapes on the projectile trajectory, a numerical firing analysis was conducted here with LS-Dyna software. Through the post-processing of this model, angular rates and transverse velocities of the projectile were determined. Due to industrial property concerns and for reasons of confidentiality, the curves submitted in this article have been normalized by dividing them by the maximum value of the results. The signals were not filtered.

2 Materials and Methods

2.1 Numerical calculation

To assess the tridimensional dynamics of the system, we developed a finite element model (FEM) with the LS-Dyna software. This code is designed to model highly dynamic phenomena with possible non-linearities due to contact, geometry, or material inhomogeneities. The study focuses on the angular and transverse velocities of the projectile.
To prevent non-convergence and aberrations of calculation, the barrel and projectile were meshed with hexahedral elements. A view of the model is presented in Figure 1. The barrel is blocked in translation in the three directions to represent the interface with the weapon near the projectile entrance. Contact between the barrel and the ammunition uses the penalty method.

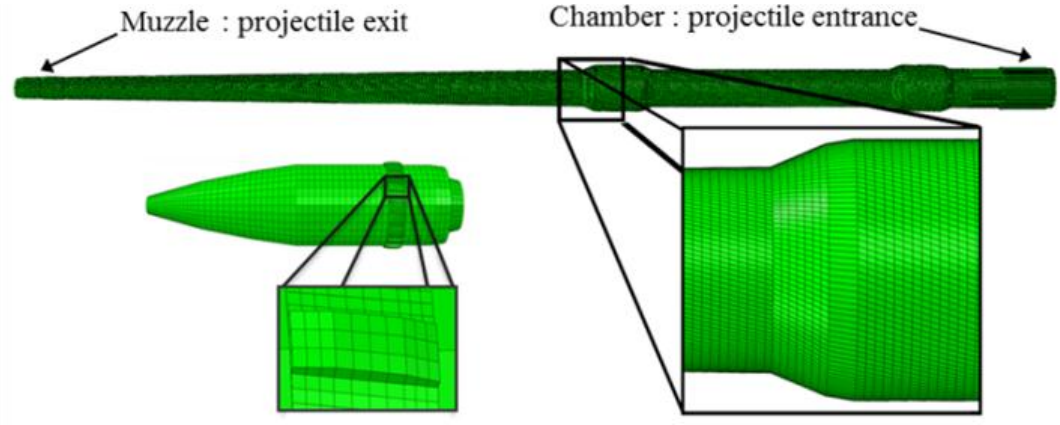

Figure 1: View of the barrel and projectile meshes.

Then the gas pressure effect on the barrel wall is added to the model using the proportional loading described by Safont [6]. The pressures and longitudinal displacement of the projectile originate from a time dependent function given by an internal ballistic code. Therefore, the tube is divided into thirty equal length segments, and the pressure curve applied on each of them is the one observed in the middle of the part (Figure 2). To finish, the ammunition travel in the barrel is defined by its displacement curve.

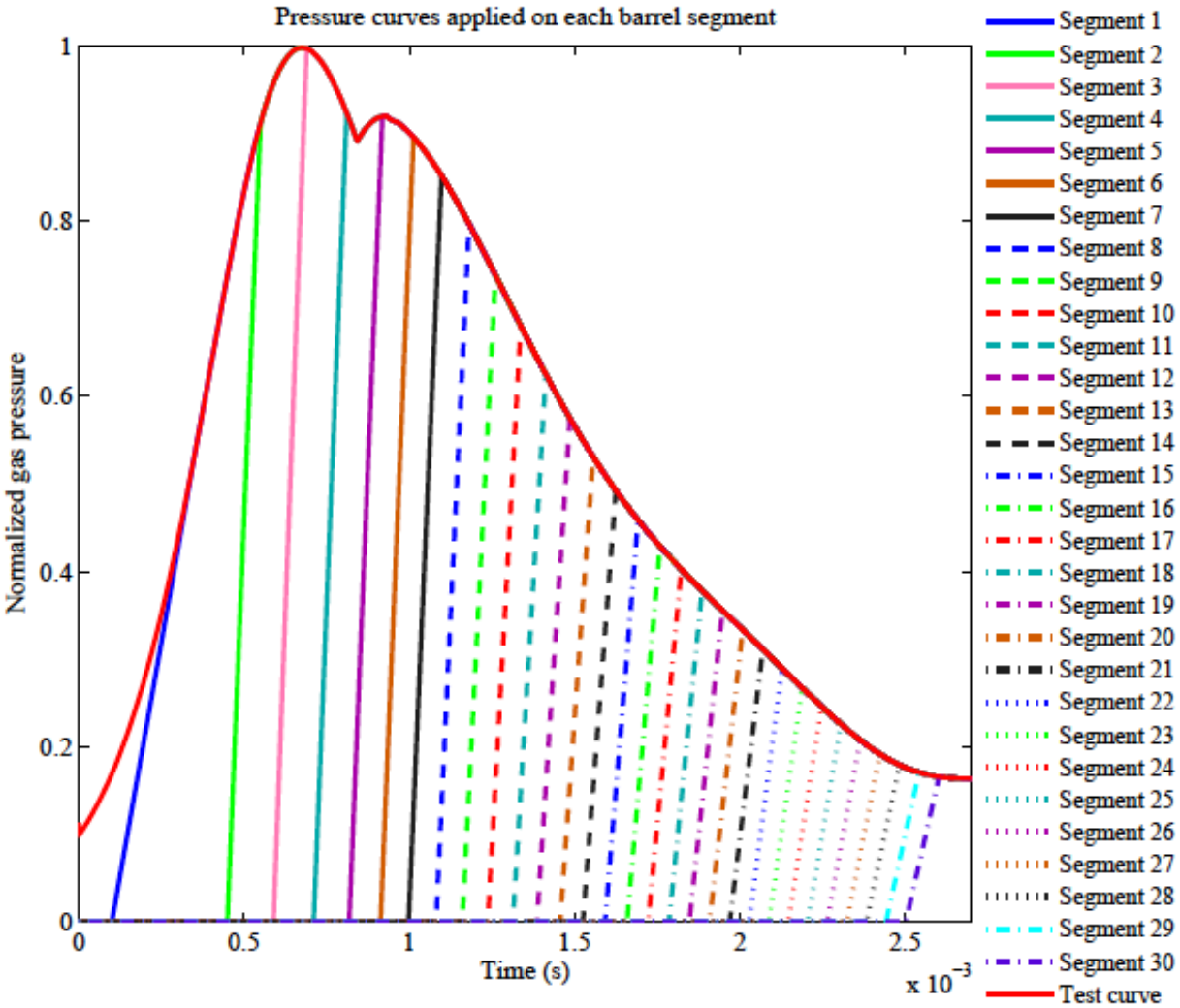

Figure 2: Gas pressure curves applied on the barrel wall.

In order to represent a straightness defect in the vertical plane, and to apply gravity, a numerical quasistatic calculation was carried out using the implicit solver of LS-Dyna. The dynamic calculation with the explicit solver was then performed using the deformed shape obtained with the quasistatic step.

Figure 3 presents the four barrel shapes used in this study. The first barrel is perfectly straight and has a deflection due to gravity. The other three have a parabolic shape. Before gravity application, the amplitude defect given to barrel 4 was three times greater than the amplitude given to barrel 2. For barrel 3, the amplitude was twice as great.

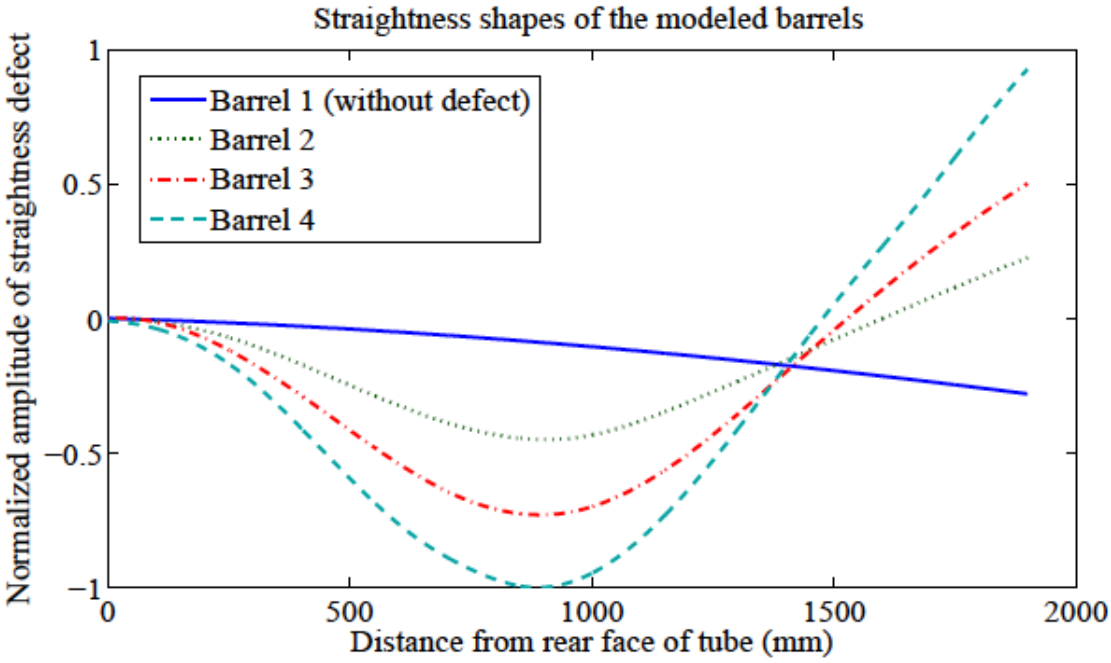

Figure 3: Straightness shapes in the vertical plane of the modeled barrels.

2.2 Circumferential strain measurements

Strain gauges were used to measure circumferential strains of the barrel as in previous tests [6]. The gauges were bonded on the external surface 680 mm from the rear face of the barrel (Figure 4). To exclude strains due to flexural stresses a Wheatstone half bridge was assembled, thus isolating circumferential strains. The results were compared with post-processing data from the dynamic calculation.

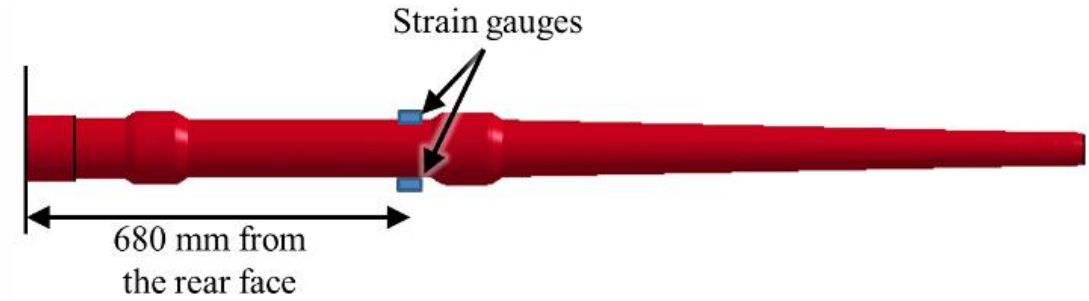

Figure 4: Strain gauges position on the tube length.

3 Results

3.1 Validation of the dynamic model

In order to use the numerical model to analyse the effect of straightness shapes is first had to be validated. Therefore, vertical deflection due to gravity, contact force between the projectile driving band and barrel, and circumferential strains were observed in order to check the representativeness of the LS-Dyna model. It is customary to measure both experimental and numerical circumferential strains in order to validate firing models [7].

To verify the vertical deflection of 0.92 mm resulting from the implicit solver, a finite element calculation was carried out using a simple conical tube with a fixed extremity. In this aim, the characteristics of mass, average inertia and volume of the true barrel were kept. With these simplifications, a maximum deflection of 0.83 mm was obtained. Thus, a 10 percent difference was observed in LS-Dyna results, which means that deflection of the quasistatic model is coherent.

Good contact logic between the projectile driving band and the barrel is essential to compute reliable numerical data. In order to check the contact, the force on the driving band surface was observed (Figure 5). The graphic exhibits a peak corresponding to the ammunition entrance. In order to ensure gas tightness, the projectile driving band has a larger diameter than that of the barrel bore, and is compressed by the tube wall. After the entrance, the contact force varied only slightly until the projectile exit, meaning that no calculation problem occurred on the tube/projectile interaction.

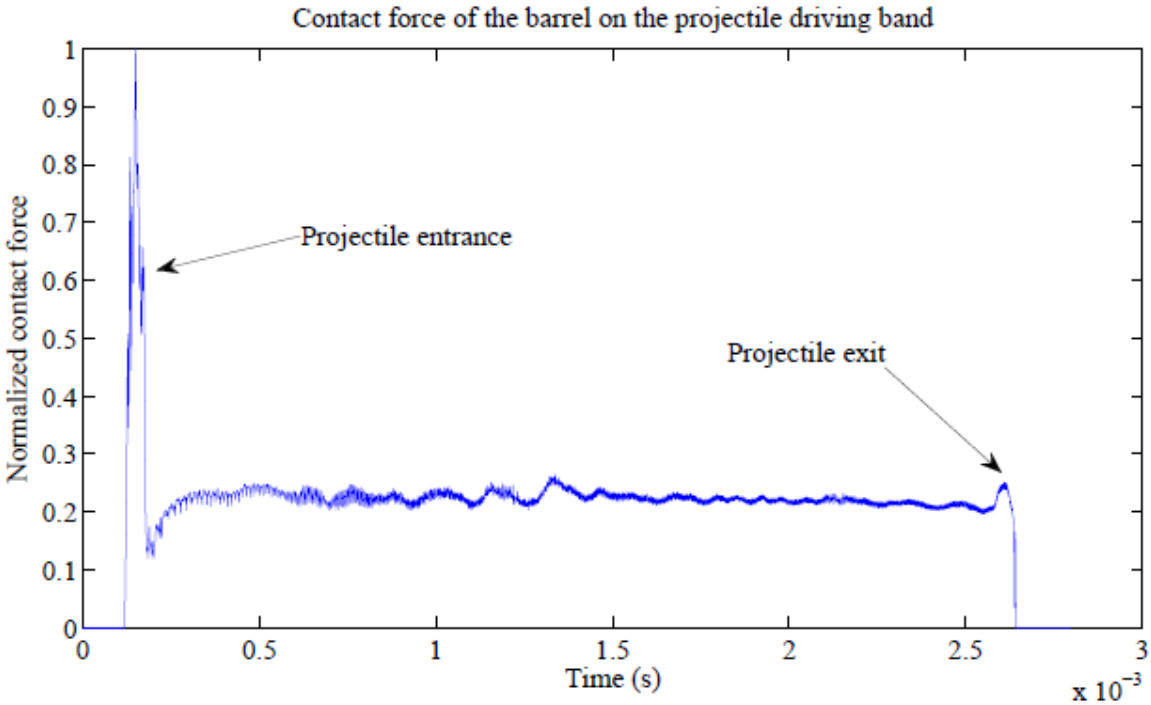

Figure 5: Contact force of the barrel on the projectile driving band.

Finally, to validate the dynamic model, circumferential strains were computed and compared with experimental results (Figure 6). The LS-Dyna peak of strain, corresponding to the driving band passage, is fourteen percent higher than that of the experimental data. This difference can be explained by the pressure which is applied shortly before the driving band passage in the model. In fact, gases are retained behind the driving band and their effect takes place just at the peak time. Thus, the peak strain slope on the LS-Dyna curve begins before the peak strain slope of the experimental results.

Considering the hypothesis of the model, the difference between experimental and LS-Dyna strains is considered acceptable.

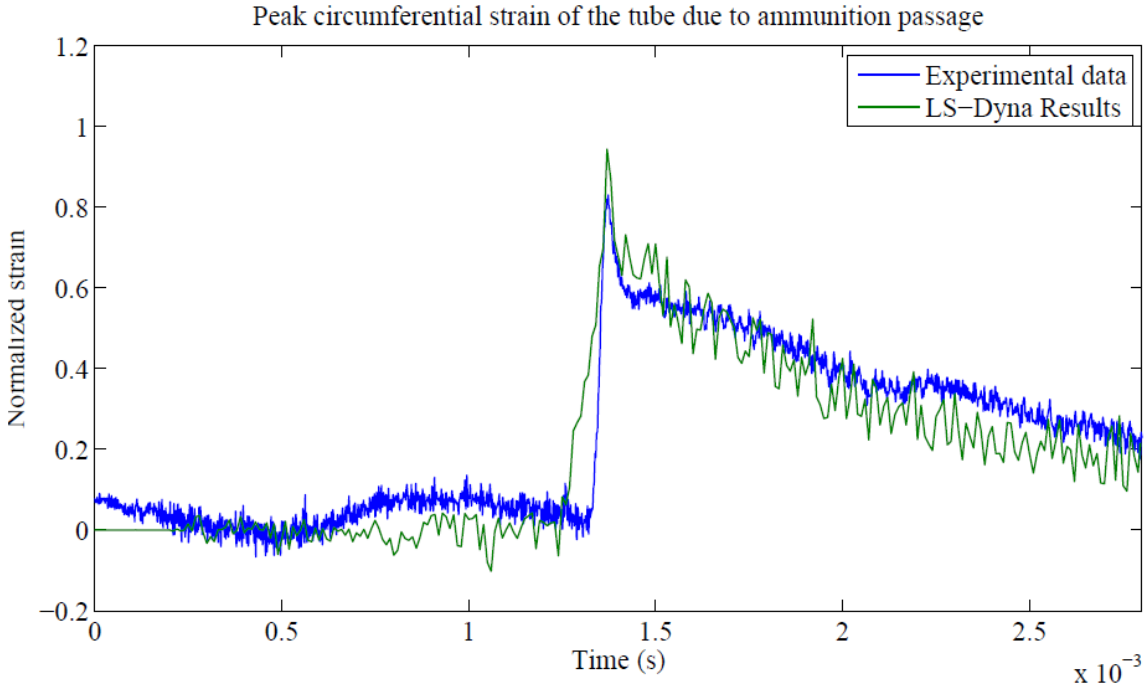

Figure 6: Comparison between experimental circumferential strains and LS-Dyna results.

Once these checks had been made, each shape presented in Figure 7 was used to calculate the dynamic response of the projectile.

3.2 Projectile exit conditions

3.2.1 Angular rates

When the projectile exits the barrel, its angular and transverse velocities depend on its in-bore travel conditions (Figure 7). Yaw rate and pitch rate were therefore observed during the projectile passage in the tube to understand the influence of different types of barrel shape. To facilitate comparison between the phenomena observed and the barrel shapes, each angular rate curve is a function of the distance from the barrel rear face. The projectile leaves the barrel 1800 mm from the rear face of the latter.

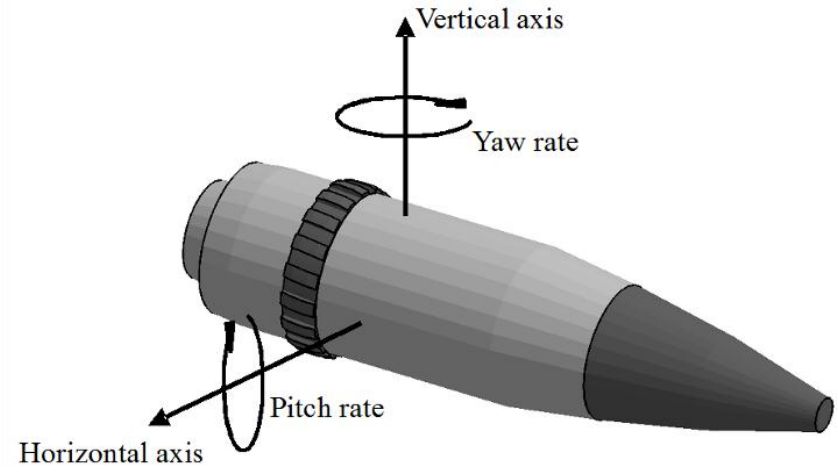

Figure 7: Yaw rate and pitch rate definitions.

Angular rates were normalized by dividing by the maximal pitch rate of the barrel 4.
Yaw rates and pitch rates of a projectile traveling in a straight barrel and one with a parabolic shape are presented on Figures 8 and 9, respectively.

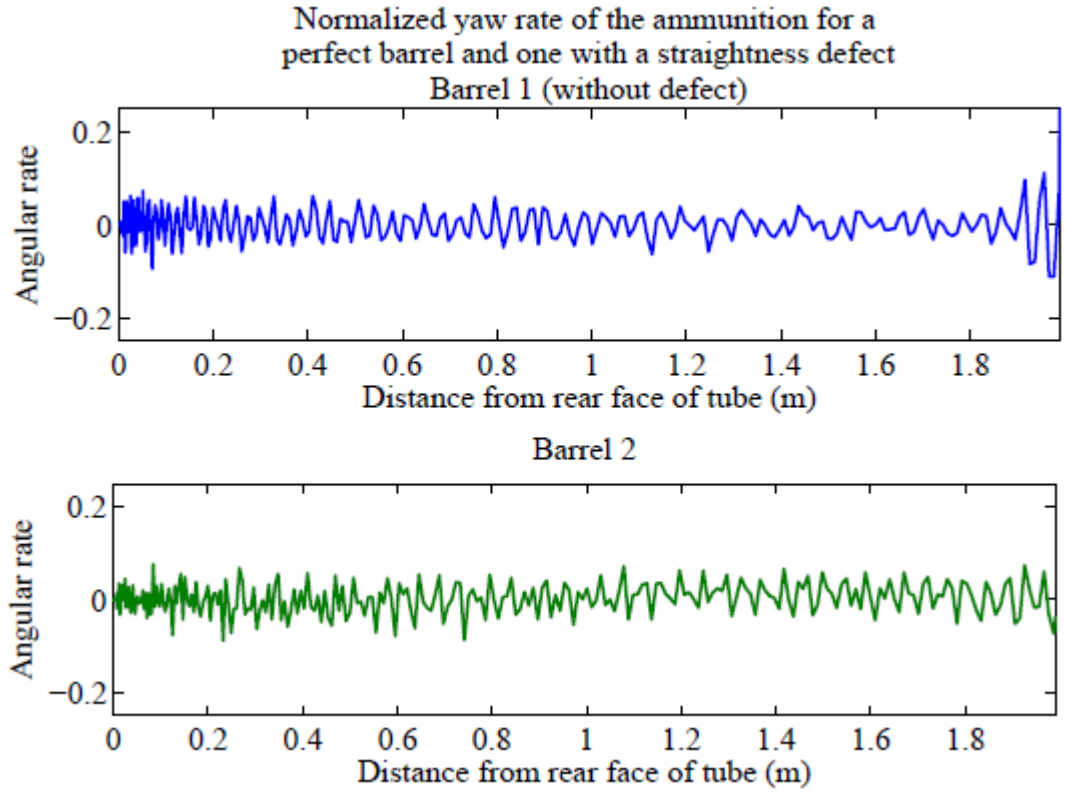

Figure 8: Yaw rate of the ammunition for a perfect barrel and one with a straightness defect.

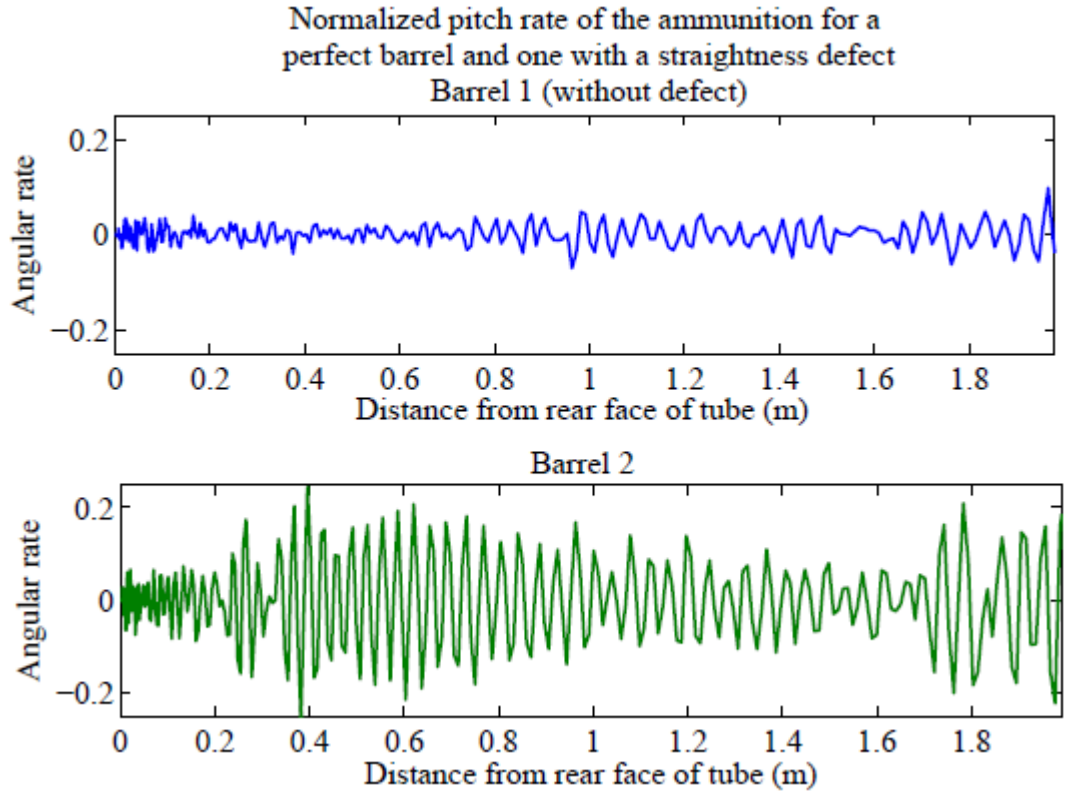

Figure 9: Pitch rate of the ammunition for a perfect barrel and one with a straightness defect.

Figure 8 shows curves close to one another, with constant amplitude and similar, but not identical, frequencies. In the barrel with a straightness defect (Figure 9), the pitch rate of the projectile is three times greater than the yaw rate whereas in the straigh barrel, the yaw rate and pitch rate are in the same order of magnitude. An increase in the pitch rate just before the barrel muzzle is observable, but the amplitude is smaller than the maximum angular velocity noted 400 mm from the rear face of the barrel.

With barrel 2, the pitch rate is the highest where the curve slope is the steepest and deviates from the tangent at the origin. Indeed 1.6 m from the rear face of the barrel, the straightness value is close to zero and the pitch rate is minimal whereas the slope is steep. Thus, the pitch rate is maximal 500 mm from the rear face.

In order to observe the influence of the amplitude of the parabolic defect, the angular velocities of barrels 2 to 4 are plotted on Figures 10 and 11. It can be seen that the angular rate frequencies are similar for the three barrels and that the pitch rates have the same shapes. However for barrel 2, the velocities are up to four times lower than for barrels 3 and 4. As previously, the pitch rate increases just before the projectile exits the tube and is higher than the yaw rate. For barrels 3 and 4, the maximum amplitudes of pitch rates are similar and occur when the projectile is close to the barrel muzzle.

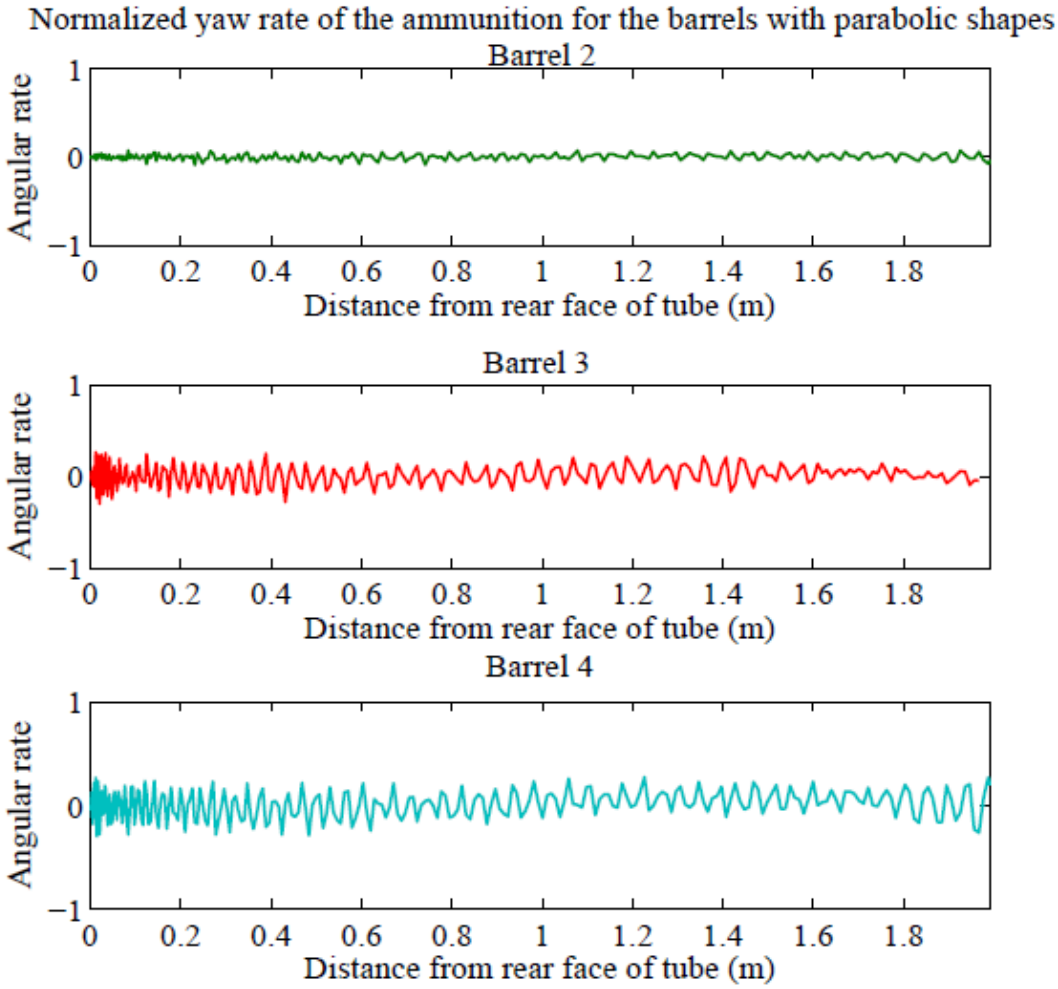

Figure 10: Yaw rate of the ammunition for the barrels with a parabolic shape.

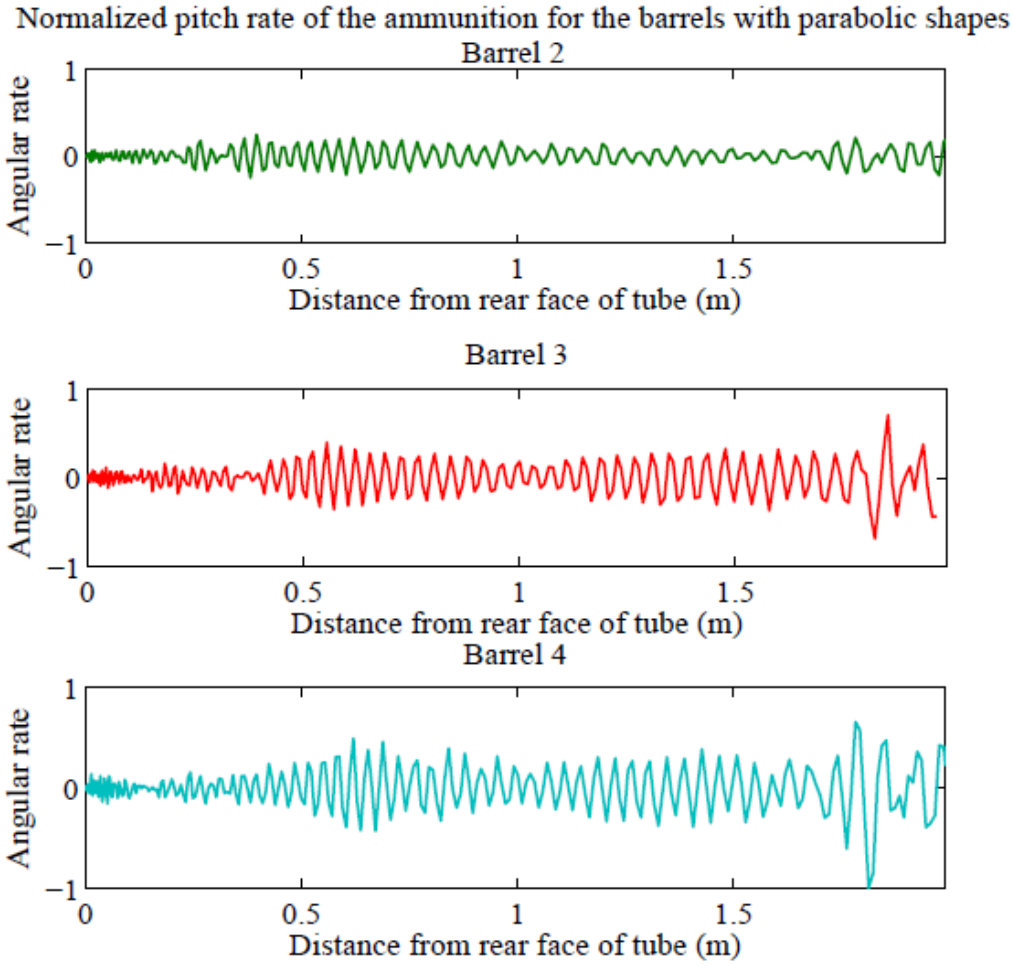

Figure 11: Pitch rate of the ammunition for the barrels with a parabolic shape.

3.2.2 Angular rates

To define the muzzle crossing velocity, it is necessary to know not only the angular rates but also the transversal velocities of the projectile until it enters the flight phase. The horizontal and vertical velocities of a perfectly straight barrel and of barrel 2 are shown on Figures 12 and 13, respectively. To compare the influence of the defect amplitude of barrels 2 to 4, Figures 14 and 15 show the horizontal and vertical velocities respectively. As previously, the curves are a function of the distance from the barrel rear face.

All the transverse velocities were normalized by dividing by the maximal vertical velocity of the barrel 4. Figure 12 shows that the horizontal velocity of the perfect barrel is slightly greater than the horizontal velocity of barrel 2. However it can be seen on Figure 13 that the vertical velocity of barrel 2 is four times greater than that of the barrel without defect. The horizontal and vertical velocities of barrel 1 have the same shape and amplitude. For barrel 2, its vertical velocity is four to five times higher than its horizontal velocity.

The Amplitudes of the horizontal velocities shown in Figure 14 are similar, while the vertical velocities (Figure 15) are much higher. The greater the straightness defect is, the higher the vertical velocities are.

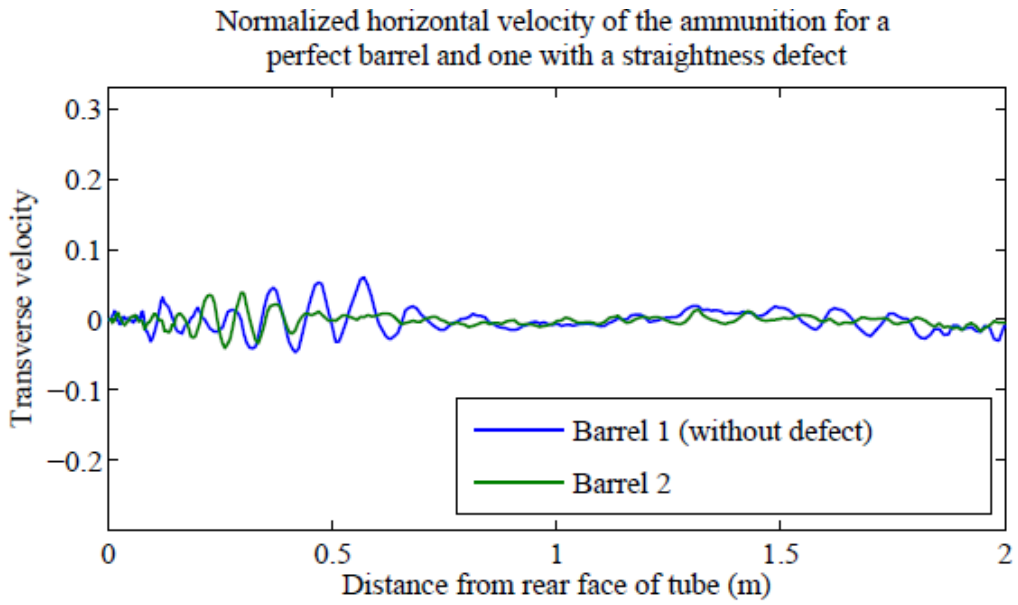

Figure 12: Horizontal velocity of the ammunition for a perfect barrel and one with a straightness defect.

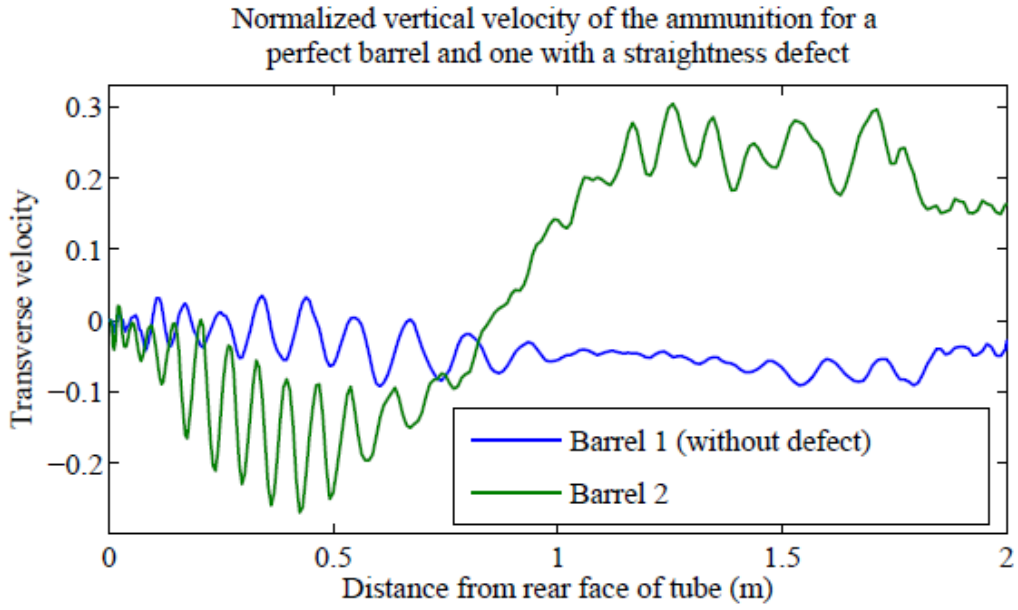

Figure 13: Vertical velocity of the ammunition for a perfect barrel and one with a straightness defect.

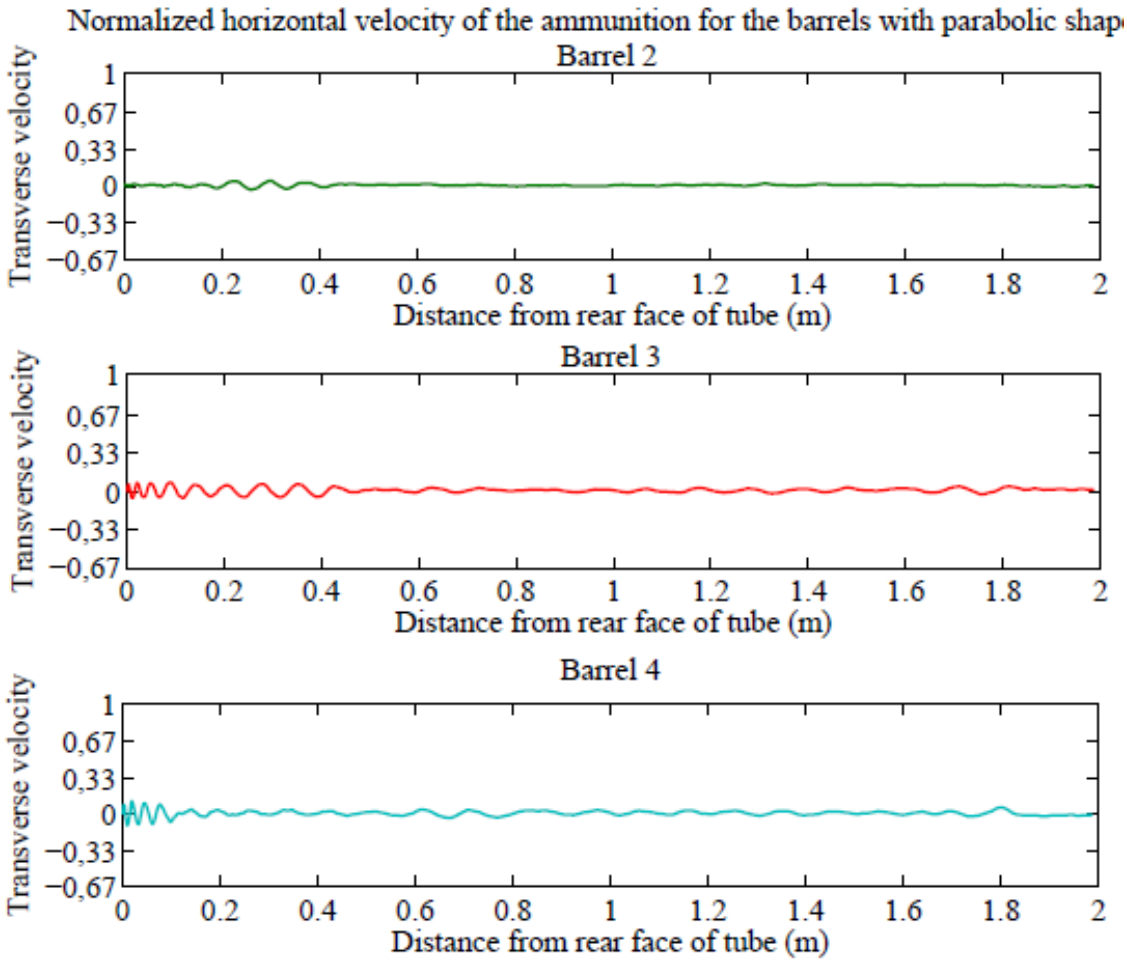

Figure 14: Horizontal velocity of the ammunition for the barrels with a parabolic shape.

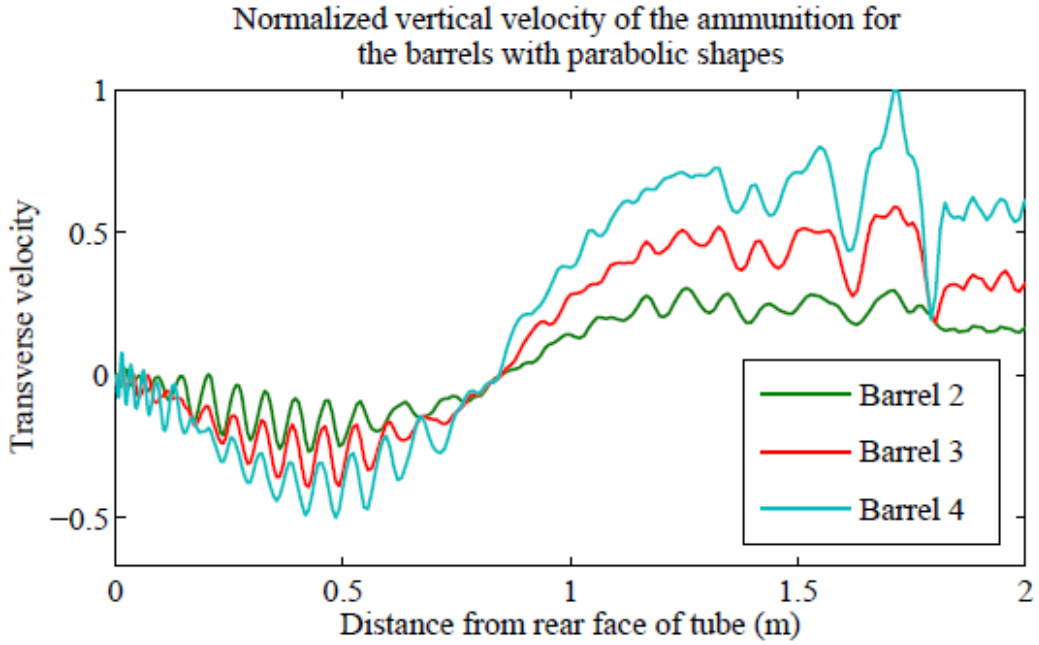

Figure 15: Vertical velocity of the ammunition for the barrels with a parabolic shape.

3 Discussion

The results obtained using the dynamic model have highlighted relationships between projectile exit conditions and barrel straightness. First of all, figures 8 to 15 show that angular rates and transverse rates are amplified in the straightness defects plane. The motion amplitudes of the ammunition are greater in the vertical plane than in the horizontal plane. Generally, the greater the straightness defects are, the more the angular velocity increases when the projectile leaves the barrel. In the case of barrel 2, angular velocity increases at the ammunition exit but the amplitude is lower than the peak observed 400 mm from the barrel rear face. For each tube with defects, a local maximum is observed at the distance from the rear face where an inflection point of the straightness curve occurs (Figure 16). The shape of the angular rate curves is related to the first and second derivative curve which represent the slope and the curvature, respectively. Even by using the simple beam model, previous works [8] have demonstrated the influence of the local slope and curvature on the tube response.

Concerning the transverse velocities of the projectile, the curves plotted in Figures 12 to 15 seem to be composed of two distinct ammunition motions. Thus, it is possible to discern a sinusoidal curve, probably due to projectile balloting, added to the trajectory imposed on the projectile following the slope of the straightness curve of the tube (Figure 16). For the barrel with defects, the amplitudes of the sinusoidal are similar in the first half of the barrel. However, near the muzzle, the greater the amplitude defect is, the more the projectile, and thus the sinusoidal, is affected by disturbances.

Previous studies conducted on total jump calculation concluded that the higher the angular rates and transverse rates are when the projectile exits the tube, the greater the aerodynamic jump is. Based on the observations made, barrel straightness appears to directly influence the exit conditions of the projectile. Thus, a barrel with significant straightness defects can amplify the total jump.

This analysis is a first approach to understanding the influence of barrel straightness on firing accuracy. Thereafter, to obtain the CG-jump it will be necessary to calculate the ratio of the barrel muzzle velocity to the projectile velocity at shot exit. To achieve this, displacements of the muzzle barrel and lateral accelerations of the projectile will be measured in order to adjust the numerical simulation. When the model is sufficiently representative of reality, the CG-jump will be calculated for different barrel geometries. The ultimate aim is to avoid the use of barrel shapes which make a significant contribution to reducing gun performances.

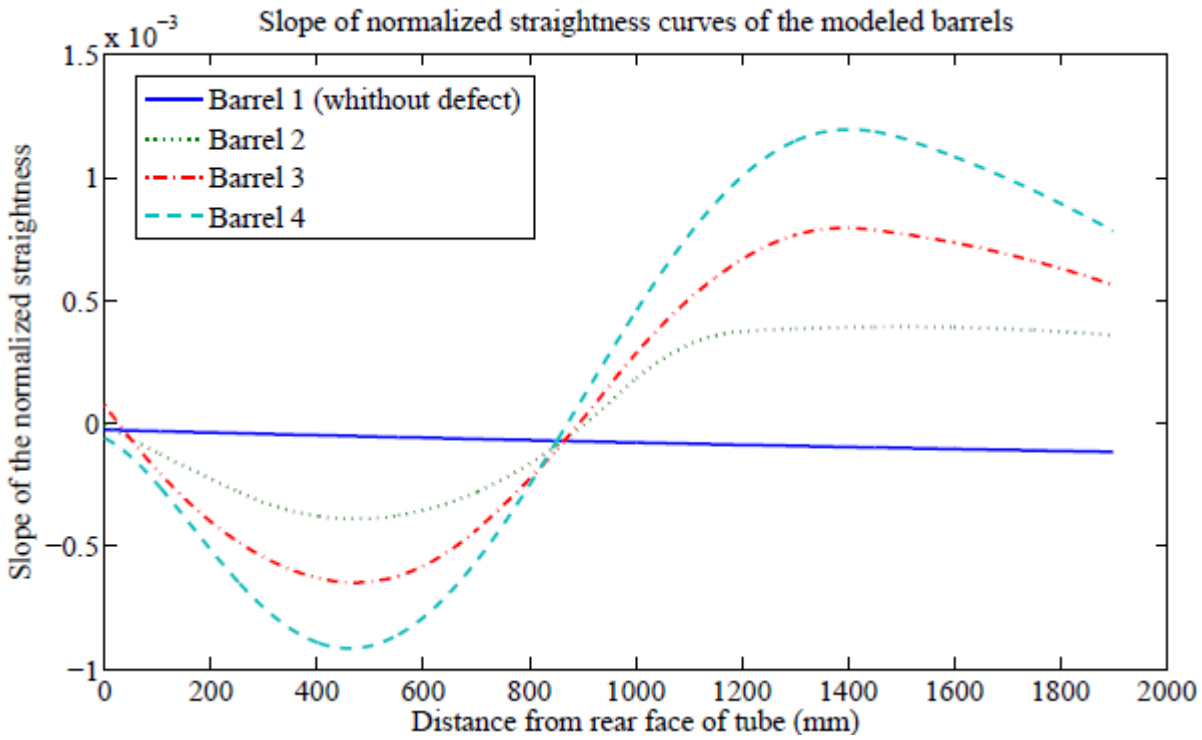

Figure 16: Slope of normalized straightness curves of the modeled barrels.

References

[1] J. Bornstein, I. Celmins, P. Plostins and E. M. Schmidt, Techniques for the Measurement of Tank Cannon Jump, Army Ballistic Research Laboratory Aberdeen Proving Ground Maryland, 1988.

[2] I. Celmins, Accuracy and Jump Measurements of the 5.56-mm M855 Cartridge, Army Ballistic Research Laboratory Aberdeen Proving Ground Maryland, 2011.

[3] M. M. Chen, Projectile balloting attributable to gun tube curvature, Journal Shock and Vibration, volume 17, 2010, pp. 39-53.

[4] J. F. Newill, B. J. Guidos and C. D. Livecchia, Comparison Between the M256 120-MM Tank Cannon Jump Test Experiments and ARL's Gun Dynamics Simulation Codes for Prototype KE, Army Ballistic Research Laboratory Aberdeen Proving Ground Maryland, 2001.

[5] J. M. Garner, B. J. Guidos, K. P. Soencksen, D. W. Webb, Flat Fire Jump Performance of a 155-mm Ml98 Howitzer, Weapons and Materials Research Directorate, Army Research Laboratory, Aberdeen Proving Ground, September 1999.

[6] O. Safont, Méthodologie de dimensionnement de tubes en dynamique, PhD Dissertation, University of Orléans and Nexter Systems, 2011, pp 157-162.

[7] A. Oger, O. Chevalier, Y. Guilmard and J. Crepin, Thermo-Mechanical Analysis of a Gun Tube During Firing, Volume 1, 28th International Symposium on Ballistics, September 24-26, 2014.

[8] Q. Lambert, A. Langlet, J. Renard and N. Eches, Dynamique en flexion de tubes parcourus à grandes vitesses, Mécanique & Industries, Volume 9, November 2008, pp 559-569.